ICSO 2016

International Conference on Space Optics

Biarritz, France

18–21 October 2016

New approaches for the design and the fabrication of pixelated filters

J. Lumeau

F. Lemarquis

T. Begou

K. Mathieu

et al.

NEW APPROACHES FOR THE DESIGN AND THE FABRICATION OF PIXELATED FILTERS

J. Lumeau[1,*], F. Lemarquis[1], T. Begou[1], K. Mathieu[2], I. Savin De Larclause[2], J. Berthon[2]

[1]Aix Marseille Université, CNRS, Centrale Marseille, Institut Fresnel UMR 7249, 13013 Marseille, France
[2]Centre National d'Etudes Spatiales (CNES), 18 av. Edouard Belin, 31401 Toulouse, France
[*]julien.lumeau@fresnel.fr

INTRODUCTION

Multispectral or hyperspectral images allow acquiring new information that could not be acquired using colored images and, for example, identifying chemical species on an observed scene using specific highly selective thin film filters. Those images are commonly used in numerous fields, e.g. in agriculture or homeland security and are of prime interest for imaging systems for onboard scientific applications (e.g. for planetology). Those instruments are generally composed with a rotating filters wheel placed inside the imaging system [1]. However, it is obvious that these rotating filters wheels are a bulky and heavy solution that make them non optimal solution for onboard applications. To overcome this problem, a solution is the fabrication of pixelated optical filters, similar to the Bayer filters used for color cameras but using specific thin film filters technologies. There have been several works over the past few years on the development of this new technology using thin film filters [2]. For example, in previous works, we presented an approach based on the deposition of multilayer filters through photolithographic masks [3]. However, combining high performances filters and small pixel size is very challenging as the filter thickness might exceed the technological capabilities of masking, and as the aspect ratio (filter thickness/pixel width) might be close to 1. In this paper we propose a new approach to overcome these problems. We first present a theoretical study of a new strategy of pixelated filters based on a dual filter approach. A complex but uniform multiband filter is used for generating all the required spectral bands. It is then associated with pixelated filters that are used to select one of these different bands. The specification for pixelated filters are thus drastically relaxed, and a thickness reduction by a factor between 2 and 3 is demonstrated. Then, an experimental demonstration of this approach before pixelating is presented by using the combination of plasma assisted reactive magnetron sputtering and plasma assisted electron beam deposition. Finally, an analysis of this approach is detailed.
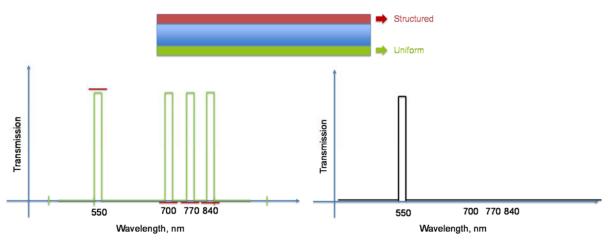
I. PRINCIPLE OF THE PROPOSED APPROACH

The simplest solution to obtain a pixelated filter corresponds to that of a single cavity Fabry-Perot structure with a pixelated cavity layer. In that case, the centering wavelength is roughly proportional to the cavity thickness, giving a multiplicative factor that takes into account the phase shift dispersion upon reflection on the cavity mirrors [4]. The fabrication is thus considerably simplified since these cavity mirrors are common to all the filters, while only one layer is pixelated, usually performed by reactive ion etching. Metal-Dielectric-Metal or all-dielectric quarter-wave Fabry-Perot structures can be used in that case but both can only result in limited performances [5]. First, the shape of the bandpass cannot be highly selective with a single-cavity structure. Second, the bandwidth and the rejection level cannot be adjusted separately since both depend on the cavity mirrors. At last, broad rejection bands are not possible with all-dielectric structures, due to phase shift dispersion on mirrors, while metal-dielectric structure are rapidly limited by absorption. For these reasons, this approach is limited to applications with relaxed spectral requirements. Considering all-dielectric multi-cavity Fabry-Perot structures can help to overcome these difficulties, but in that case, several layers need to be pixelated, which considerably increases the complexity of the manufacturing process.

As a consequence, when more challenging spectral characteristics are required, the approach consists in a discrete Bayer-type structure. In that case, each spectral band corresponds to a specific thin film stack. This can be achieved by sequentially depositing the complete filters through a photolithographic mask and perform a lift-off of the photoresist in order to eliminate the filter on the undesired regions and obtain pixels of filters [6]. While this approach is very promising, it shows severe limitations as soon as one wants to improve the filter performances since it rapidly increases the filters thicknesses, with respect to the pixel size. Indeed, obtaining a narrower bandpass or a more square profile is associated with increasing either the number of layers of the mirrors

and/or the number of cavities, while increasing the rejection level and/or bandwidth also requires increasing the number of layers of the blocking mirrors and/or the number of blocking mirrors. As a matter of fact, it is worth noting that for many advanced applications, e.g. the case of the fabrication of filters with bandpass with a square profile of a few tens of nanometers within a rejection region covering all the silicon detector sensitivity (400-1100 nm) and a good signal to noise ratio (SNR) higher than 20 or 40 (i.e. ratio between in-band and out-band fluxes), the total thickness of the filter will be between 5 and 20 μm, depending on the exact requested performances. One can see that even in the case of the thinnest filters, obtaining a filter with a micropixel size of 5 μm (in accordance with actual CCD or CMOS cameras) will results in cubic pixels with an aspect ratio defined as the ratio between the thickness and the lateral size of the pixel, equal or higher than 1 and therefore not compatible with actual photolithographic fabrication capabilities.

In this approach all the filters are deposited and pixelated on a common face of the filtering component, which requires to pixelate the total thickness of rather thick complex filters. To overcome this limitation we propose, as illustrated in Figure 1, a dual-face approach, one face being coated with a common filter, the other with pixelated filters that are expected to be thinner:

- The uniform side (i.e. not pixelated) is used to generate a filter that provides all the specified spectral bands, with the required specifications, as well as the specified rejection level between these band-pass.
- The second face is coated with a pixelated filter that selects one of these band-pass and rejects the others. For these filters, the band-pass characteristics can be highly relaxed since full specifications are answered by the common filter, while the rejection characteristics are spectrally limited to the other band-pass. An immediate result is that the filters to be pixelated will have a lower thickness.

Fig. 1. Illustration of the new approach for pixelated filters. Top: a scheme of the filter, bottom left the spectral profiles of the uniform 4-band filter and of one of the pixelated filters to select the band at 550 nm, bottom right the spectral profile of the filter resulting from the combination of one of the pixelated and the uniform filter.

II. DESIGN OF THE UNIFORM 4-BAND AND PIXLATED FILTERS

We considered the design of pixelated filters with following parameters:

- The 4 bandpass filters have central wavelengths 550, 700, 770, and 840 nm.
- FWHM is about 40 nm
- Transmission in the bandpass is higher than 80%
- Rejection is performed in 500 – 900 nm range
- Signal to noise ratio is higher than 20

If the classical approach for band-pass designs is based on the use of quarter-wave stacks, this is no more possible for multiple band-pass filters with an arbitrary spacing between the different bands. For this reason, all the filters have been designed numerically using the so-called needle technique [7]. Such design technique allows obtaining a stack formula with any physically-valid spectral profile, usually with a lower total thickness that classical quarter-wave coatings which is an advantage for our purpose, but with arbitrary layer thicknesses which can add complexity for thickness monitoring during manufacturing. However, when associated with stable

deposition processes, and efficient monitoring techniques, this design technique can lead to the manufacturing of complex filters with any profiles such as a landscapes [8] or a moose head [9] have been reported.

We first designed the uniform 4-band filter that allows generating the four bandpass and the rejection level out of those ones. We considered a couple of high and low refractive index materials (i.e. Nb_2O_5 and SiO_2) and used the refractive index dispersions that are commonly obtained with a Plasma Assisted Reactive Magnetron Sputtering (PARMS, Bühler/Leybold Optics HELIOS machine) [10]. Spectral profile of the designed filter is shown in Figure 2.
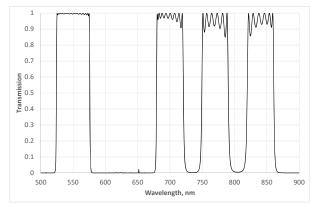

Fig. 2. Spectral profile of the uniform four-band filter that was designed.

The filter is composed with 97 alternated high and low refractive index layers associated with a total thickness of 9.4 μm. While such a filter is far from being trivial to fabricate, it is however compatible with actual PARMS technology [9].

The second step was the design of each of the four pixelated filters that allow sequentially selecting each of the four considered bands. For this design, we considered a couple of high and low refractive index materials (i.e. Nb_2O_5 and SiO_2) and used the refractive index dispersions that are commonly obtained with a Plasma Assisted Electron Beam Deposition (PA-EBD, Bühler/Leybold Optics SYRUSpro 7110 machine) [11]. Actually, as the PARMS technology is not compatible with the deposition through photolithographic masks due to its geometry (sample/target distance of a few centimeters and extended targets size), we considered a different deposition technology, for instance PA-EBD, which secures a large target/sample distance (for instance 600 mm) and small shadowing effects when depositing through the mask. Table 1 shows the parameters and the performances of the filters in terms of SNR when both uniform 4-band and pixelated filters are combined.

Tab. 1. Parameters and the performances of the filters in terms of SNR when both uniform 4-band and pixelated filters are combined.

	Total thickness (μm)	Number of layers	SNR	FW @ 80% (nm)
B1 filter 525-575 nm	1.917	18	20.14	51
B2 filter 680-720 nm	2.329	25	25.17	40
B3 filter 750-790 nm	3.094	31	27.61	39
B4 filter 820-860 nm	2.218	26	27.14	40

One can see that pixelated filters with total thickness between 2 and 3 microns allow obtaining, after combination with the uniform 4-band filter, performances matching the requirements. As a comparison, achieving the same performances with a single side approach as the one that was used up to now [3], requires depositing filter with thickness within 5 to 10 microns. In other words, this new approach allows decreasing the thickness of the filters to be pixelated by a factor equal to 2 to 3 and the required thicknesses are then more compatible with the production of pixelated filters with a micropixel size within 5×5 μm². Figure 3 illustrates the spectral profiles of the uniform four-band filter and the four pixelated filters that were designed while Figure 4 shows the spectral profiles of the filter resulting from the combination of the uniform 4-band and the pixelated filters both in linear

and in logarithmic scales (the resulting transmittance is calculated taking into account of the multiple reflections that occur between the uniform and the pixelated filters). One can see that the rejection is very high and defined by the uniform 4-band filter far from the main bandpass regions. The overall rejection is thus limited by the rejection level of the bands that were not selected by the pixelated filters. In other words, increasing the rejection band to the whole silicon band would only require increasing the thickness of the uniform 4-band filter but would not affect the thickness of the pixelated filter, while increasing the SNR would mainly require increasing the thickness of the pixelated filter. It is also worth noting that the B3 filter is surrounded by two close bandpass. Eliminating the B2 and B4 bandpass requires a larger thickness than the other filters which have just one (or no for B1) close bandpass to be rejected.
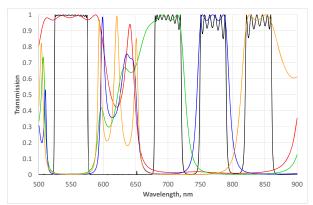

Fig. 3. Theoretical spectral profiles of the uniform four-band filter (black curve) and the four pixelated filters (colored curved) that were designed.
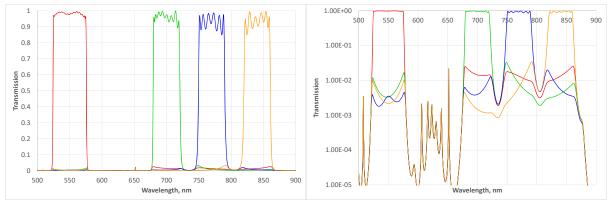

Fig. 4. Theoretical spectral profiles of the filters resulting from the combination of the uniform 4-band and the pixelated filters both in linear (left) and in logarithmic (right) scales.

III. EXPERIMENTAL DEMONSTRATION OF THE PERFORMANCES OF THE PROPOSED APPROACH

Before performing a complete demonstration of the proposed approach combining deposition and structuring of the filter, we first demonstrated that the designed structures can be well reproduced using actual deposition technologies. Each of the filters were fabricated within the *Espace Photonique* technological platform of the *Institut Fresnel*. PARMS technology using a Bühler/Leybold Optics HELIOS machine was used for the fabrication of the uniform 4-band filter while PA-EBD technology using a Bühler/Leybold Optics SYRUSpro 710 was used for the fabrication of each of the four filters to be pixelated. For all filters, the thickness of each layer was controlled by optical monitoring using a Bühler/Leybold Optics OMS 5000 system.

Regarding the uniform 4-band filter, we defined an optimal strategy for the optical monitoring of the filter. Since the design does not exhibit any periodicity and therefore tends to be very sensitive to deposition errors, we used a similar approach as the one we recently reported [9]. It is based on the decomposition of the design into sub-stacks and the use of different monitoring glasses for each of these sub-stacks. This approach is possible with the HELIOS machine thanks to the load-lock that allows replacing the monitoring sample being coated by a new one, without opening the whole deposition chamber and therefore without affecting the other samples being coated.

An analysis using a Virtual Deposition Process software that simulates the deposition allowed defining a monitoring strategy based on 6 test glasses associated with 6 changing monitoring wavelengths:

- Layers 01-12: 575 nm
- Layers 13-30: 555 nm
- Layers 31-46: 580 nm
- Layers 47-62: 505 nm
- Layers 63-82: 460 nm
- Layers 83-97: 580 nm

One can see that the monitoring wavelengths are all within the same region of the spectrum around 550 nm, but the fine adjustment of those one associated with a regular change of the monitoring glass were shown to secure minimum errors on the thickness of each layer not exceeding ±1%. After fabrication, the complete 4-band filter was characterized using a Perkin Elmer Lambda 1050 spectrophotometer. Figure 5 shows the theoretical and experimental transmission profiles of the filter in the 500-900 nm region. One can see that both profiles show very good agreement with deviation in transmission not exceeding ±5%. The long wavelength bands are slightly shifted to longer wavelength, e.g. by about 2.5 nm at 750 nm, i.e. 0.3%. This error is small and could be corrected by further improving the monitoring strategy or by a refinement of the dispersion curves of the deposited materials. As a matter of fact one can see that the monitoring wavelength are within the 550 nm region resulting in a filter properly centered at this wavelength. One can then expect that by a selecting a broader range of monitoring wavelengths, this deviation could be minimized.
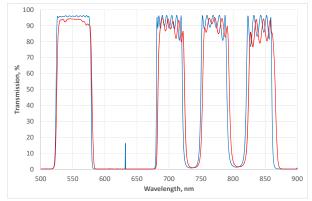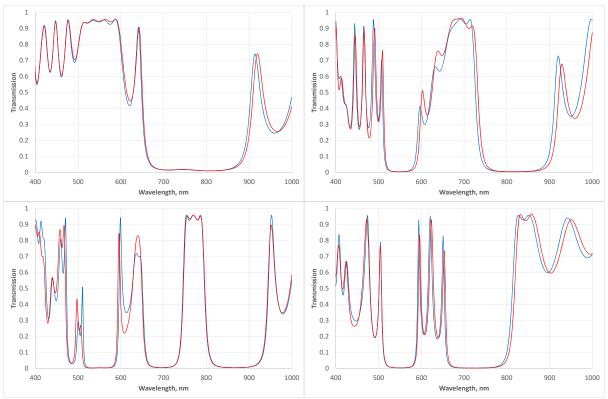

Fig. 5. Spectral profile of the uniform 4-band filter. In blue, the theoretical profile and in red the experimental profile.

We then fabricated each of the filters to be pixelated. At this stage, we only deposited uniform filters having the designs of Table 1 using PE-EBD. Similarly to the first filter, we defined optimal optical monitoring strategies for each of the filter. These strategies are based on one or two different monitoring wavelengths for each filter, with a single monitoring glass since monitoring glass could not be changed during deposition using this technology and no change was required due to the lowest complexity compared to the 4-band filter. After fabrication, each of the four filters was characterized using a Perkin Elmer Lambda 1050 spectrophotometer. Figure 6 shows the theoretical and experimental spectral transmission of each of the filters in the 500-900 nm region.

Fig. 6. Spectral profile of each of the filters to be pixelated. Top Left: B1 filter, Top right: B2 filter, bottom left: B3 filter and bottom right: B4 filter. In blue, the theoretical profile and in red the experimental profile.

One can see a very good agreement between experimental and theoretical data confirming that minimal errors have been achieved during the fabrication of each of the filters. The spectral deviation of each of the filters is equal or lower than the one that were obtained on the 4-band filters (i.e. below 0.5%), confirming that the designs are highly compatible with actual deposition technologies.

Finally, using the combination of the spectral profiles of both uniform 4-band filter and each of the filters to be pixelated, we simulated the performances of the final filters (Figure 7). One can see that despite a slight smaller transmission, of a few percent, at the valley of the transmission bands oscillations, high performances filters can be achieved with a very good agreement between theory and experiment.
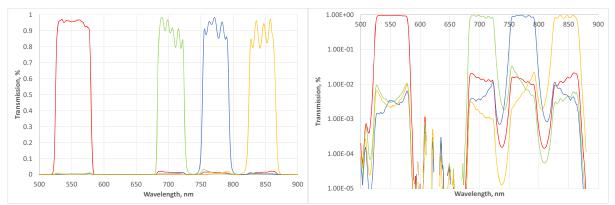

Fig. 7. Experimental spectral profiles of the filters resulting from the combination of the uniform 4-band and the pixelated filters both in linear (left) and in logarithmic (right) scales.

CONCLUSIONS

We presented in this paper a new design and fabrication strategy for the development of pixelated filters. It is based on a dual filter approach. A complex but uniform multiband filter is used for generating all the required spectral bands. It is then associated with pixelated filters that are used to select one of these different bands. We first presented the general approach and the designs that allow achieving the requested spectral performances.

Then, the proposed filters designs were experimentally demonstrated by using the combination of plasma assisted reactive magnetron sputtering and plasma assisted electron beam deposition. We showed that high performances filters can be achieved. Using this new strategy, we showed that the specification for pixelated filters are thus drastically relaxed, and a thickness reduction by a factor between 2 and 3 is achieved. Based on this technique, the thicknesses of the filters to be pixelated do not exceed 3 μm and are thus more compatible with obtaining small pixel size using actual photolithographic technique. Experimental demonstration of such a pixelated filter is ongoing.

REFERENCES

[1] H. Krol, F. Chazallet, J. Archer, L. Kirchgessner, D. Torricini, C. Grèzes-Besset. "Narrowband filters for Ocean Colour Imager," ICSO - 7th International Conference on Space Optics – 2008.

[2] George Themelis, Jung Sun Yoo, and Vasilis Ntziachristos, "Multispectral imaging using multiple-bandpass filters," Opt. Lett. **33**, 1023-1025 (2008).

[3] M. Lequime, L. Abel-Tiberini, J. Lumeau, K. Gasc, J. Berthon, "Complex Pixelated Optical Filters", International Conference on Space Optics (Tenerife, Spain), paper 66454, October 2014.

[4] M. Lequime, R. Parmentier, F. Lemarchand and C. Amra, "Towards Tunable Thin-Film Filters for Wavelength Division Multiplexing Applications," Appl. Opt. **41**, 3277-3284 (2002).

[5] B. Portier, F. Pradal, M. Oussalah, H. Sik, J. Fleury, and P. Laprat, "Pixelated Thin Film Coating on Detector for Multispectral Infrared Imaging," in Optical Interference Coatings 2016, OSA Technical Digest (online) (Optical Society of America, 2016), paper MC.8.

[6] J. M. Eichenholz, "Dichroic Filter Array Multispectral Imaging Systems," in Imaging and Applied Optics Congress, OSA Technical Digest (CD) (Optical Society of America, 2010), paper ATuA4.

[7] A. V. Tikhonravov, M. K. Trubetskov, and G. W. DeBell, "Optical coating design approaches based on the needle optimization technique," Appl. Opt. **46**, 704-710 (2007).

[8] J.A. Dobrowolski, S. Browning, M. Jacobson and M. Nadal, "Topical Meeting on Optical Interference Coatings (OIC' 2001): Manufacturing Problem," Appl. Opt. **41**, 3039-3052 (2002).

[9] T. Begou, F. Lemarchand and J. Lumeau, "Advanced optical interference filters based on metal and dielectric layers", Optics Express **24**(18), 20925–20937 (2016).

[10] T. Begou, H. Krol, D. Stojcevski, F. Lemarchand, M. Lequime, C. Grezes-Besset, J. Lumeau, "Complex optical interference filter with stress compensation", Optical Systems Design 2015, Proc. SPIE **9627**, paper 96270R (Jena, Germany), September 2015.

[11] H. Hagedorn; M. Klosch; H. Reus; A. Zoeller, "Plasma ion-assisted deposition with radio frequency powered plasma sources", Proc. SPIE **7101**, Advances in Optical Thin Films III, 710109 (25 September 2008).